heritage

MDPI

Article

Early Degradation Behavior of Amber-Based Paint Layers in *The Temptation of St Anthony* by Salvador Dalí

Catherine Defeyt [1,2], Francisca Vandepitte [2,3], Philippe Walter [4], Edène Derzelle [1], Nathan de Vries [1], Daniela Aleccia [1,5], Francesca Caterina Izzo [5] and David Strivay [1,*]

1 Centre Européen d'Archéométrie, UR Art, Archéologie, Patrimoine, Université de Liège, 4000 Liège, Belgium; catherine.defeyt@uliege.be (C.D.); ederzelle@uliege.be (E.D.); ndevries@uliege.be (N.d.V.)
2 Royal Museums of Fine Arts of Belgium, 1000 Brussels, Belgium; francisca.vandepitte@fine-arts-museum.be
3 Histories of Art, Architecture and Visual Culture, Vrije Universiteit Brussel, 1050 Brussels, Belgium
4 Laboratoire d'Archéologie Moléculaire et Structurale, CNRS-Sorbonne Université, 75005 Paris, France; philippe.walter@sorbonne-universite.fr
5 Department of Environmental Sciences, Informatics and Statistics, Ca' Foscari University of Venice, 30173 Venice, Italy; fra.izzo@unive.it
* Correspondence: dstrivay@uliege.be

Abstract

The iconic Dali's painting *The Temptation of St. Anthony* dated 1946, housed in the Royal Museums of Fine Arts of Belgium since 1965, displays worrying surface conditions in specific areas, notably the figure of St. Anthony. The problematic paint layers similarly exhibit uneven transparency and a rugged surface irrespective of their color, raising questions about whether these features reflect deliberate artistic intent or material degradation. To evidence potential degradation mechanisms and to identify the associated painting materials, Dali's picture has been investigated through a large panel of imaging and analytical techniques, including digital microscopy, MA-XRF, Raman and FT-IR spectroscopies, XRD and Py-GC–MS. The obtained results were subsequently assessed against the material and technical information collected from Dali's *50 Secrets of Magic Craftsmanship*, as well as against archival photographs. By combining historical and multi-analytical approaches, it was possible to diagnose the altered condition of the artwork, but above all to determine when and how the deterioration patterns took place. Visible changes of appearance occurred prior to 1965 and were most probably already initiated during the curing and drying processes of the paint films. The present study tends to demonstrate the key roles of mobile resin acids from amber, reactive zinc oxide pigment suspected of containing crystal defects, uncured lead-white-rich underlayers, and chlorine environmental contamination, regarding the early and peculiar degradation behavior observed on Dali's masterpiece.

Keywords: Dali; degradation; amber; Blockx; non-invasive

Academic Editors: Christos Karydis, Eleni Kouloumpi and Agathi Anthoula Kaminari

Received: 28 December 2025
Revised: 15 February 2026
Accepted: 16 February 2026
Published: 22 February 2026

1. Introduction

Salvador Dalí executed *The Temptation of St. Anthony* (Figure 1) in 1946 as part of the *Bel Ami International Art Competition* held in New York, ultimately won by Max Ernst [1,2]. The version of St. Anthony by Ernst dated 1945 is now conserved at the Lehmbruck Museum in Duisburg, Germany. The Salvador Dalí's *Temptation of St. Anthony* has been housed in the Royal Museums of Fine Arts of Belgium (RMFAB) since its acquisition in 1965. This emblematic work by the Catalan surrealist artist presents both conservation challenges and

unresolved questions in technical art history. Of particular concern is the heterogeneous appearance of the painting's surface, notably variations in transparency and gloss, which raise critical interpretive issues. These visual inconsistencies may either reflect deliberate aesthetic choices intrinsic to Dalí's creative process or result from deterioration phenomena affecting the pictorial layers.

Figure 1. Salvador Dalí, *The temptation of St. Anthony*, 1946, oil on canvas, 89.5 cm × 119.5 cm, Royal Museums of Fine Arts of Belgium (Inv. 7223). Photography: CEA (ULiege) ©Fundació Gala-Salvador Dali/SABAM Belgium.

To differentiate between the artist's original intentions and unintended visual alterations induced by aging or material instability, the painting was subjected to an in-depth technical and analytical study. A suite of complementary imaging and analytical techniques was employed to characterize the materials and assess their current condition. The scientific findings were subsequently contextualized through a comparative study of historical photographic documentation—dated 1946, 1947, and 1965—and critically interpreted in reference to *50 Secrets of Magic Craftsmanship* [3], a technical treatise authored by Dalí in 1947 and published in 1948.

2. Materials and Methods

A comprehensive high-resolution photographic campaign was undertaken to document *The Temptation of Saint Anthony* under both visible and ultraviolet illumination. Image acquisition was carried out using the scanning system developed by the Centre Européen d'Archéométrie (CEA) [4], equipped with a Nikon D7500 DSLR camera and an AF-S Micro Nikkor 105 mm lens. Each image covered a 4 cm × 3 cm area, achieving a spatial resolution of 8 µm per pixel. To ensure seamless image alignment and coverage, adjacent captures were taken with a 15% overlap. The resulting images were subsequently stitched into high-resolution mosaics using PTGui software, with a minimum of 20 manually defined control points per overlap to enhance geometric fidelity and stitching accuracy.

Microscale surface examination was facilitated using Dino-Lite portable digital microscopes, offering variable magnifications from ×20 to ×250, enabling detailed observation of localized surface phenomena and film morphology.

Elemental mapping was conducted through macro-X-ray fluorescence (MA-XRF) spectroscopy to identify and spatially characterize the elemental composition. The whole painting surface was analyzed using the CEA's MA-XRF platform [5,6], comprising a Moxtek Magnum X-ray tube (Ag anode) and an Amptek X-123SDD silicon drift detector (70 mm^2 active area; 130 eV resolution at Mn K_α). Scans were performed with a 1 mm step size and a dwell time of 300 µs per point. The X-ray source was operated at 40 kV and 120 µA. Data processing and elemental deconvolution were executed in batch mode using PyMCA software [7], allowing for precise visualization of pigment distributions.

Raman spectroscopy (RS) was employed for molecular characterization using an Enwave Optronics I-Dual-G portable Raman analyzer, equipped with a 785 nm excitation laser [8,9]. Three spectra were acquired at each of the selected sites, with laser power limited to approximately 30 mW to minimize thermal effects. Post-processing of the spectral data was performed using Spectragryph software [10].

Fourier Transform-Infrared spectroscopy (FT-IR) was performed using the Bruker ALPHA FT-IR spectrometer operating over the 400–4000 cm^{-1} range with 2 cm^{-1} resolution. The reflectance module enables contact-free analysis of surfaces with a 5 mm diameter spot size, ideal for identifying varnishes, binders, and degradation products.

X-ray diffraction (XRD) was used to characterize structural patterns with the setup from LAMS (Laboratoire d'Archéologie Moléculaire et Structurale, Sorbonne Université-CNRS) [11]. Measurements were performed in reflection mode using a microsource delivering a Cu K_α (8.04 keV) X-ray beam focused at a distance of 53 cm from the output of multilayer optics (from Xenocs, Grenoble, France). The beam size was 200 µm × 800 µm with an angle of about 8° between the painting surface and the beam. Diffracted X-rays were detected with the Mythen 2 linear detector (Dectris, Baden-Daettwil, Switzerland, 1280 channels) during 10 min. The signal was then processed to obtain XRD patterns and interpreted using the Bruker Eva software.

Additionally, micro-fragments from Dalí's painting were investigated through pyrolysis–gas chromatography–mass spectrometry (Py-GC-MS). Py-GC-MS analyses were performed by Ca'Foscari University (Venezia) in collaboration with the Institute for Natural Science and Technology in the Arts of the Academy of Fine Art of Vienna. A Py-GC-MS in double-shot (DS) mode was selected, which is based on a two-step analysis [12]: thermal desorption (TD) of the samples at a lower temperature to detect volatile compounds, and thermally assisted hydrolysis and methylation-based pyrolysis (Py) of the same sample as the second step by adding 2 µL of tetramethylammonium hydroxide (TMAH) reagent (25 wt% aqueous solution of TMAH, Sigma Aldrich, Milwaukee, WI, USA). NIST 05 and NIST 05 s Library of Mass Spectra were used to identify the compounds.

All imaging and non-invasive analytical work was conducted in situ at the RMFAB, using a mobile laboratory setup. This approach allowed for non-invasive investigation with minimal stresses to the artwork, while maintaining high analytical accuracy and methodological consistency.

3. Results and Discussion

3.1. Diagnosis of the Altered State

A comparative examination between the earliest available black-and-white photograph of *The Temptation of St. Anthony*, taken shortly after its completion in 1947 [13], and the painting's current condition reveals the significant increased transparency that occurred in some places (Figure 2). The changes are confined to specific pictorial elements—such as the figure of Saint Anthony and his rock, the building of El Escorial, the flying angel, the elephant bringing up the rear, and the pinkish tower this one carries on his back—each of which appears to have been executed in the final stages of the painting process. These

items display a combination of surface irregularities, including uneven transparency and pronounced textural roughness, irrespective of their color (Figure 3).

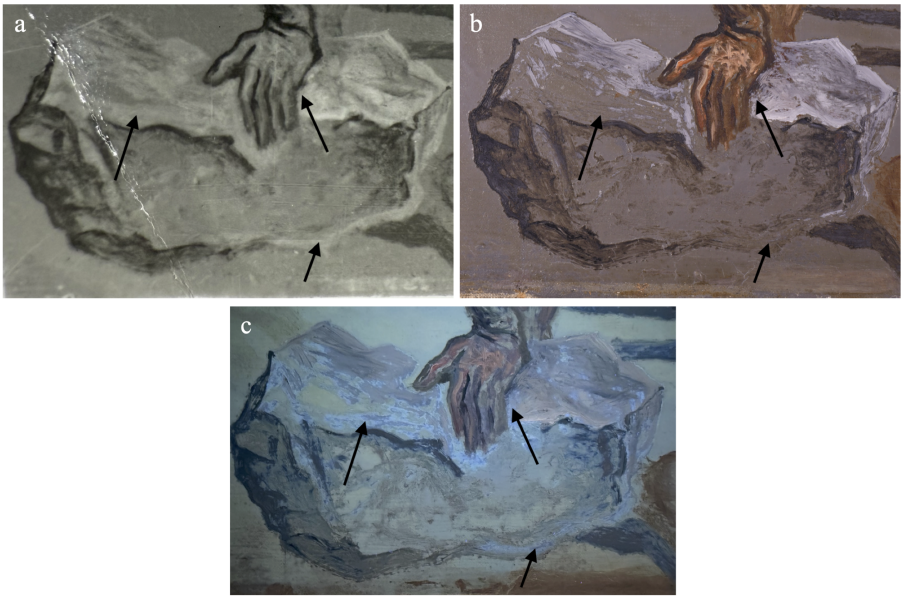

Figure 2. Detail of the rock on which the Saint leans from. (**a**) 1947 B&W photo. (**b**) 2024 visible photo. (**c**) 2024 photo under UV light. Arrows point to zones with modified transparency.

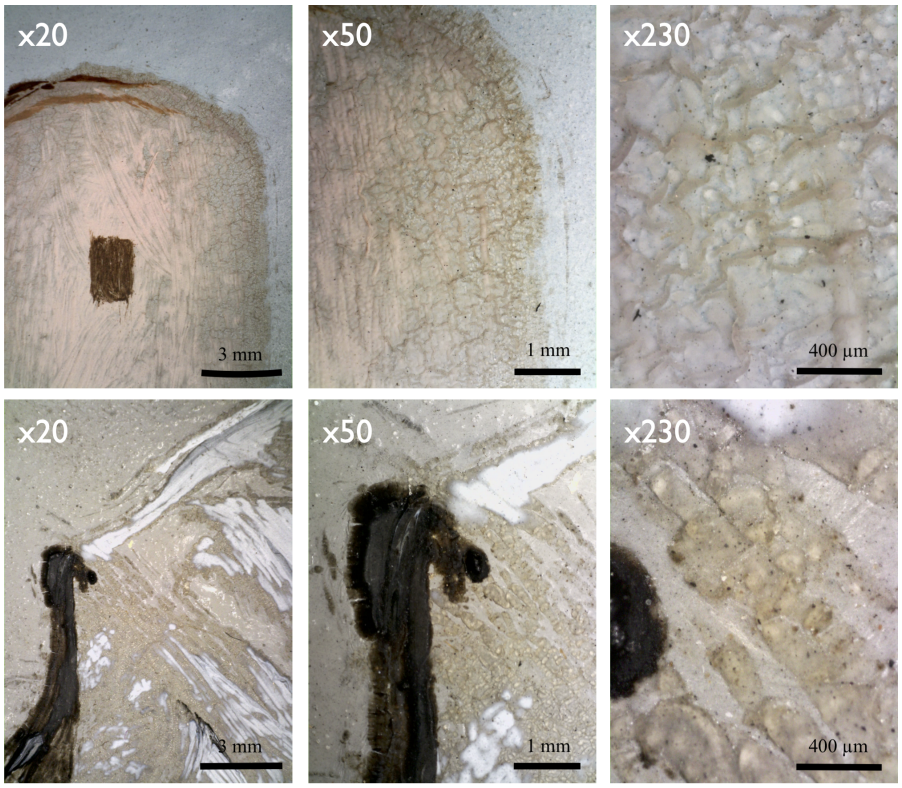

Figure 3. Microphotographs of degraded paint films from the pinkish tower (**above**) and from the rock supporting St. Anthony (**below**).

A shared characteristic among these degraded areas is their distinct bluish-white luminescence under ultraviolet (UV) illumination, which starkly contrasts with the surrounding regions that exhibit a lower-intensity purplish-blue emission (Figure 2c). This luminescence behavior may indicate alterations of the binding medium related to zinc-ion migration

and the creation of vacancy defects, which could affect the photoluminescence intensity of zinc oxide [14]. Further examination by digital microscopy confirmed significant structural disruption within the paint films, manifesting as micro-cracking and translucent crusts (Figure 3). These film failures underscore the severe deterioration of the binder.

Importantly, comparison with a color photograph dated 1965, which is the date of painting acquisition by the RMFAB, demonstrates that these changes in appearance occurred within two decades of the painting's creation. The early onset of such degradation suggests intrinsic material instability or problematic stratigraphic interactions from the outset, rather than the result of natural aging alone.

3.2. Painting Materials

3.2.1. Pigments

To effectively elucidate the degradation mechanisms affecting *The temptation of St. Anthony* and to identify the associated reaction products, it was first essential to characterize the painting materials and technique employed by Salvador Dalí. The comprehensive understanding of the pigment-binder mixtures and the inferred layering served as the foundation for interpreting the chemical and physical changes observed in the work.

The pigments were characterized through MA-XRF analysis of the whole painted surface, complemented by spot analyses using Raman spectroscopy (Figure A1) and X-ray diffraction (Figure A6). Based on the overall results obtained, the palette used for St. Anthony incorporates the following pigments: strontium yellow ($SrCrO_4$), Ceruleum blue ($CoSnO_3$), cobalt blue (Al_2CoO_4), various chromium-based greens, carbon black, earthy pigments, lead white combining cerussite ($PbCO_3$) and hydrocerussite ($2PbCO_3{\cdot}Pb(OH)_2$), and zinc white (ZnO) (Table 1). These last three pigments were also identified by XRD (Figure A6). The original ground layer consists of drying oil combined with titanium white in the anatase phase (TiO_2) and anhydrite ($CaSO_4$) (Figure A5). Except for strontium yellow, all identified pigments are in line with the artist's recommendations found in his treatise *50 Secrets of Magic Craftsmanship* [3]. Indeed, Dalí explicitly advised against the use of strontium yellow, considering it unsuitable for artistic purposes. The questioning presence of this pigment may be attributed to confusion caused by misleading or inconsistent commercial naming conventions at the time.

Table 1. Identified pigments with the corresponding analytical technique. Elements are given for XRF, bands and spot analysis (#) for RS (see figures for Raman identification).

Pigment	Formula	XRF Elements	RS Bands (cm^{-1}) [#]
Strontium yellow	$SrCrO_4$	Sr, Cr	862, 893 [2]
Ceruleum blue	$CoSnO_3$	Co, Sn	-
Cobalt blue	Al_2CoO_4	Co	-
Ultramarine	$Al_6Na_8O_24S_3Si_6$		547 [1]
Chromium green		Cr	-
Carbon black	-		1315, 1590 [2]
Earthy pigments	Fe_2O_3 and MnO_2	Fe, Mn	-
Cerussite	$PbCO_3$	Pb	1048 [3]
Hydrocerussite	$2PbCO_3{\cdot}Pb(OH)_2$	Pb	1048 [3]
Zinc white	ZnO	Zn	432 [4]
Anatase	TiO_2	Ti	140 [5]
Anhydrite	$CaSO_4$	S, Ca	1017 [5]

The elemental distribution maps generated through MA-XRF (Figures 4–6), particularly the zinc (Zn) distribution, provided critical insight into the spatial correlation between

material composition and degradation patterns. It was observed that the zones exhibiting pronounced surface alteration are consistently associated with high concentrations of zinc white. However, not all areas containing zinc white are affected. A key distinction emerged: only those zinc-white-rich paint layers that are superimposed over lead white-containing layers display visible signs of deterioration (Figure A4). This stratigraphic configuration is fully compliant with *50 Secrets of Magic Craftsmanship*—which described Dalí's preference to use zinc white at the end of the process, in the uppermost paint layers.

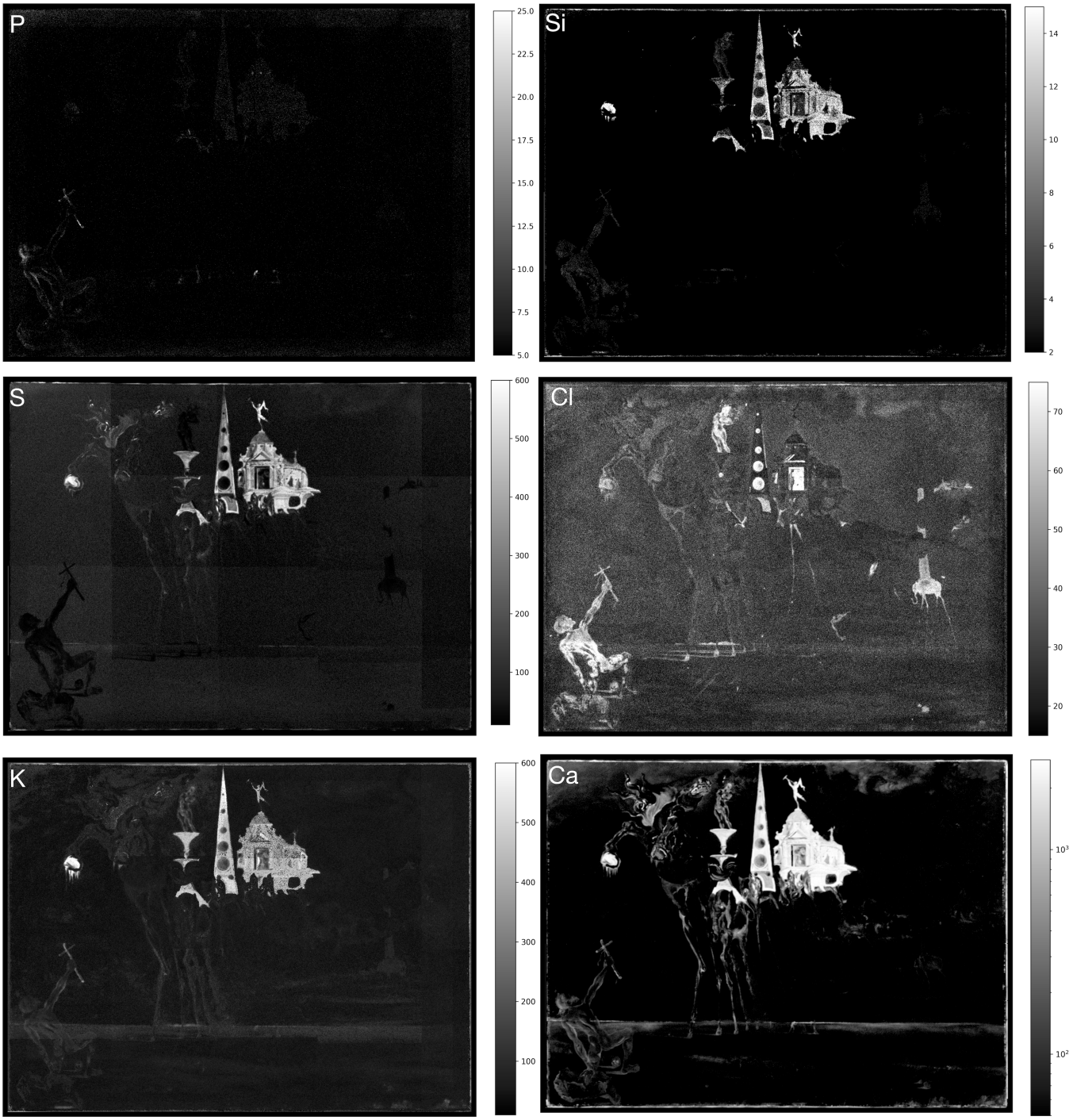

Figure 4. MA-XRF distribution maps of phosphorus (P), silicon (Si), chlorine (Cl), potassium (K) and calcium (Ca).

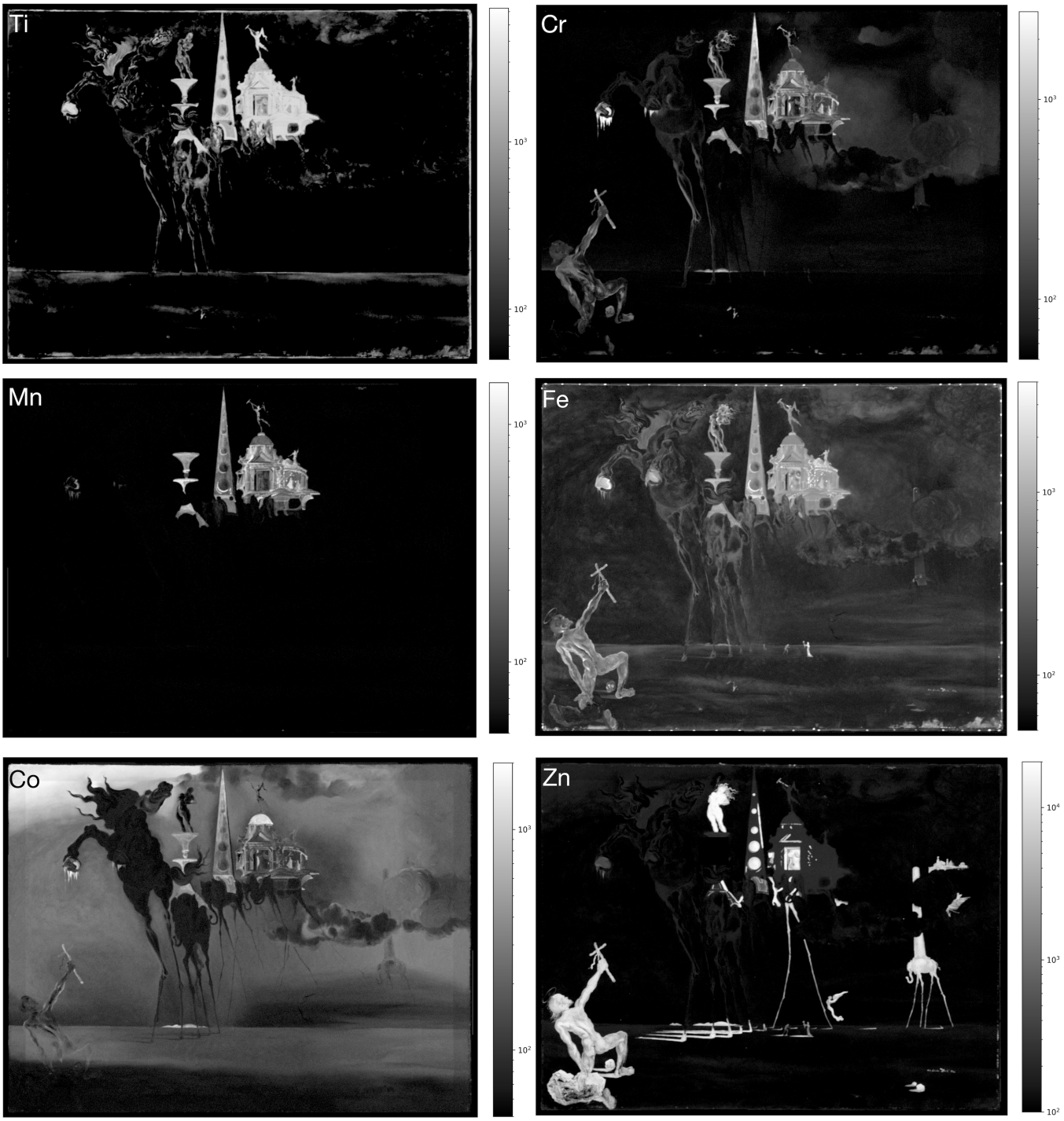

Figure 5. MA-XRF distribution maps of titanium (Ti), chromium (Cr), manganese (Mn), iron (Fe), cobalt (Co) and Zinc (Zn).

In contrast, zinc white-containing colors applied directly onto the original ground layer show no discernible signs of degradation (e.g., in the female figure on top of the front elephant). This finding indicates that the interaction between the zinc white top layers and lead white underlayers may have played a key role in the degradation process of the upper layers. Another element is the drying/curing issues affecting the lead-white-based layer, as evidenced clearly by the presence of wrinkles following the contours of the items painted above (Figure 7).

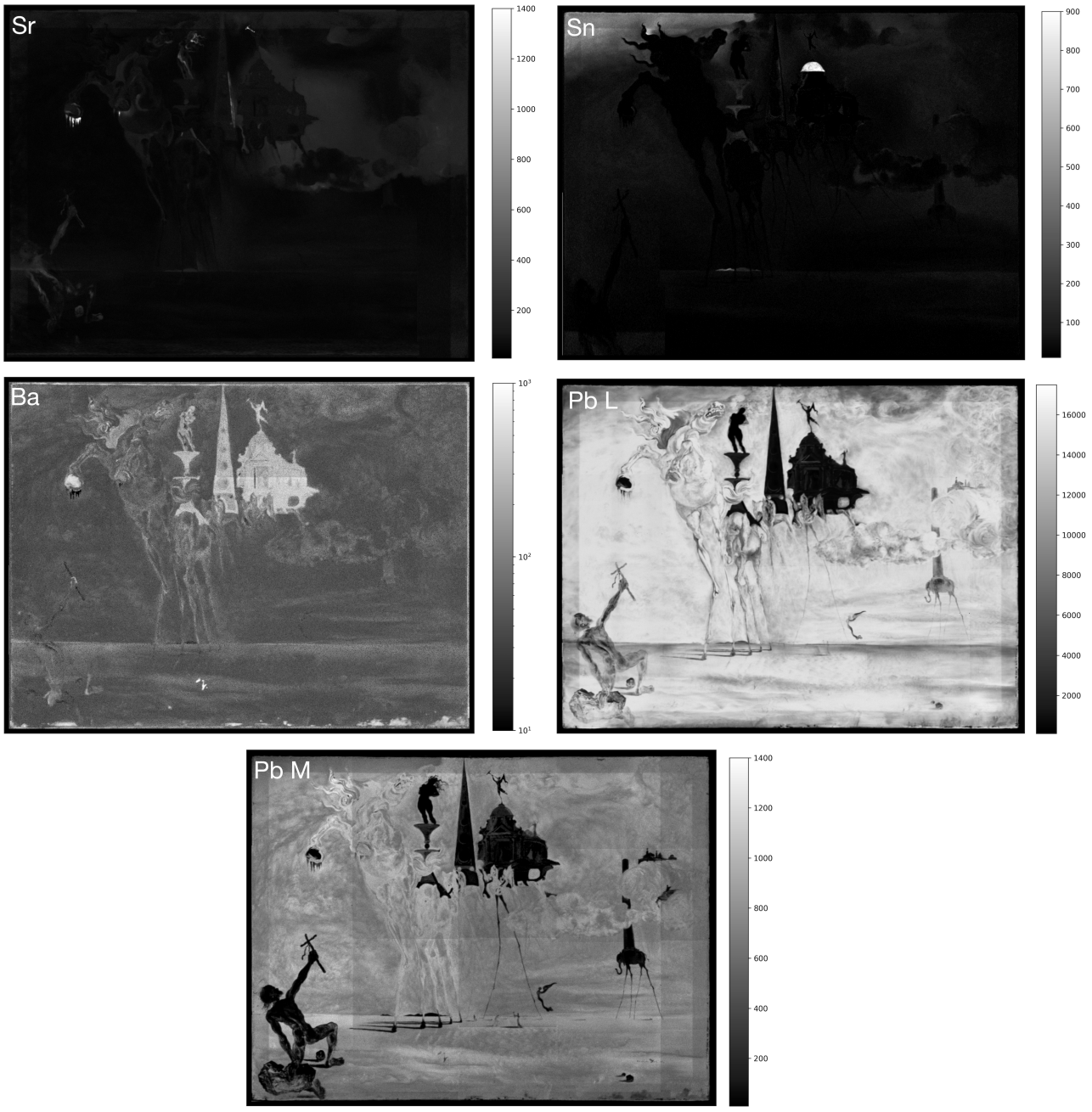

Figure 6. MA-XRF distribution maps of strontium (Sr), tin (Sn), barium (Ba), and Lead (Pb L and M lines).

Although the reactivity of zinc white pigments in oil-based paint systems and the related saponification of fatty acids are well documented [15], the specific degradation features seen in *The temptation of St. Anthony*—transparency and surface roughness—do not correspond to the usual zinc soap protrusions widely covered by the literature [16]. In contrast, lead-white-based underlayers display typical lead soaps protrusions. In any case, the presence of lead-white-rich layers underneath appears to have played a key role in the degradation behavior of superimposed layers, possibly through catalysis or other ionic interactions at layer interfaces.

An additional element of interest is the widespread detection of chlorine (Cl) across the painted surface (Figure 4). Chlorine signals detected on the overall picture are unlikely to originate from the constitutive materials. By contrast, it is highly probable that chlorine represents an exogenous contaminant introduced after execution. Supporting this hypothe-

sis, chlorine contents were also detected on the original wooden frame through spot XRF measurements (Figure A7), suggesting environmental exposure rather than material origin. This implies that the artwork was at some point exposed to chlorine compounds, such as chloride ions from the seawater environment.

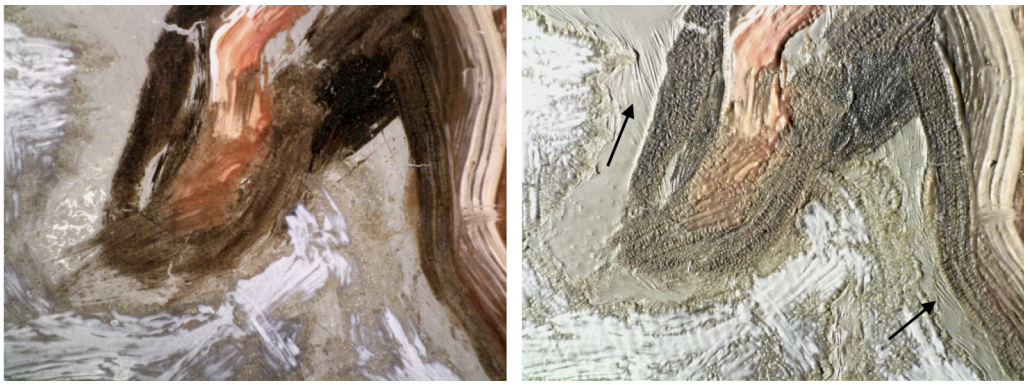

Figure 7. Macro-photographies in visible (**left**) and raking light (**right**) showing the wrinkles of the lead-white-based film following the contours of the figure of St. Anthony and his rock, painted above, providing clear evidence of drying/curing issues.

Interestingly, while chlorine was detected across the painting surface, the highest concentrations consistently coincided with areas rich in zinc white, regardless of whether these regions were visibly degraded. This spatial correlation may be explained by the chemical affinity of zinc compounds for halides, potentially promoting the retention or accumulation of chloride ions within the zinc-containing layers [17].

In summary, the deterioration phenomena observed for *The temptation of St. Anthony* involve interactions between zinc white and the underlying lead white layer, and probably an environmental chlorine contamination.

3.2.2. Mediums

Salvador Dalí regarded binding mediums as the quintessence of what constitutes "good" painting, placing particular emphasis on their role in achieving desired viscosity, optical depth and invisible brushstrokes. Among all mediums, amber held a privileged status in his practice. In *50 Secrets of Magic Craftsmanship*, Dalí describes amber in exalted terms:

> "At this point I must put my hand on my heart and confess to you sincerely that my whole experience of thirty-five years as a painter has convinced me that it is an error to mix with the precious oils of your overpainting any kind of varnish or solvent whatsoever, and that the sole really precious vehicle which for the first time in this book I permit myself to call 'sublime' is the yellow liquid amber according to the formula arrived at by Jacques Blockx, which you dissolve in your oils at the beginning of your overpainting in the proportion of one drop of amber to five of oil, and which you augment progressively up to the end of the picture."

Amber is a fossil resin resulting from the natural polymerization and fossilization of exuded plant resin over millions of years. The most well-known amber is Baltic amber, believed to be produced by Pinites succinifer (extinct conifer species) and mineralogically known as succinite. It is mainly found in the "Blue Earth" formations on the Baltic coast [18,19] and it has the typical behavior of a high-molecular-weight crosslinked polymer. According to Théodore Turquet de Mayerne, the Flemish masters from the 15th and 16th centuries were the first to succeed in dissolving amber [20].

From a chemical perspective, Baltic amber is characterized by the presence of the dicarboxylic acid succinic acid (1,4-butanedioic acid) in both free and esterified forms, occurring

in approximately equal proportions [21,22]. This distinctive feature has led to its designation as succinite. The fraction of free carboxyl groups imparts ion-exchange resin–like behavior to the polymer, whereas esterified succinic acid promotes crosslinking, resulting in a higher average molecular weight, elevated melting point, and reduced solubility.

Overall, Baltic amber exhibits the typical properties of a high–molecular-weight, crosslinked polymer and can be regarded as a natural alkyd resin. It is essentially formed through the esterification of a polyvalent alcohol (a copolymer derived from communol and communic acid) with a dicarboxylic acid, namely succinic acid [23].

In addition, the soluble portion of amber contains identifiable monoterpenoids and diterpenoids. The monoterpenoid fraction includes compounds such as borneol, camphor, fenchyl alcohol, and fenchone, as well as derivatives like fenchyl and bornyl hemisuccinates. The diterpenoid fraction comprises, besides succinic acid, minor amounts of acid esters typical of fresh conifer resins, including 48-iso-pimaric acid (approximately 0.4% *w*/*w*), whose persistence over millions of years is noteworthy.

Jacques Blockx (1844–1913), whom Dali praises (Figure 8a), was a Belgian artists' color maker who developed, in the 1860s, an original process to dissolve amber, and for which he was awarded during the Exposition Universelle held in Paris, in 1878. The amber-based painting solutions and varnishes prepared according to Blockx recipes (Figure 8b) basically consist of mixtures of dissolved amber and drying oils, in variable proportions [24].

Figure 8. (**a**). Portrait of Jacques Blockx with dedication by S. Dali reproduced in *50 Secrets of Magic Craftsmanship*: *Ce monsieur qui n'a jamais peint procurera plus aux peintres de demain, que ce que nous avons accompli, tous les peintres modernes réunis. Le dernier à savoir comment il fallait peindre* (This man, who has never painted, will provide more to the painters of tomorrow than all that we modern painters together have accomplished. The last one to know how painting should be done). (**b**). Historical specimens of amber-based mediums and varnishes produced from Blockx conserved at the CEA (University of Liège).

Regarding *The temptation of St. Anthony*, the presence of amber within the pictorial layers has been analytically confirmed. Indeed, Py-GC-MS analyses were carried out on two micro-samples from different areas (Figure A3). The first sample is from the grey ground and has two layers (pictorial layer, ground layer). The second sample is from the light-grey cloud with glossy appearance and dark grains in one pictorial layer. The Py-GC-MS analyses (Figure 9) permitted identifying succinic acid (1,4-butanedioic acid), characteristic of Baltic amber [23]. The use of Baltic amber is consistent with the Py-GC-MS results obtained for fresh, amber-based solutions from the Blocxk company (*Solution à peindre 25 mL*), analyzed in the same experimental conditions [12].

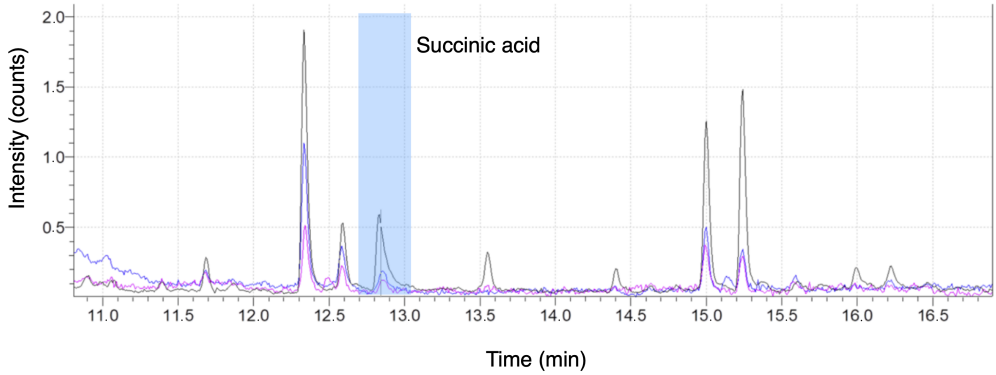

Figure 9. Detection of the main marker of Baltic amber, succinic acid (1,4-Butanedioic acid), through Py-GC-MS pyrograms of two micro-samples taken from Dali's painting (in blue and pink) and of fresh, amber-based solution from Blockx (in black).

Natural resins, while offering desirable optical and mechanical properties, are also known to exhibit complex and sometimes problematic aging behavior in the presence of certain inorganic pigments. Previous studies [25–28] have documented the susceptibility of terpenoid resins to degradation catalyzed by metal ions, particularly zinc. These ions promote the formation of metal–resin acid complexes, which may alter the solubility, stability, and optical characteristics of paint films over time.

In Dalí's painting, the co-occurrence of amber-rich media and zinc white in the upper layers is, therefore, of relevance. The affinity of zinc ions for resin acids likely led to the formation of zinc–resinate complexes, which may affect the original properties of the paint films. Such interactions could be responsible, at least in part, for the observed irregularities in gloss, transparency, and surface texture noted in affected areas of the painting. The study of laboratory-prepared mockups would be of great interest to verify this assumption. The detection of amber in *The temptation of St. Anthony* not only corroborates Dalí's written instructions and aesthetic intentions but also introduces a critical variable in understanding the painting's current condition. The interplay between amber-based binder and zinc white pigment appears to be a key factor in the degradation phenomena observed.

3.2.3. Degradation Products

Based on the analytical identification of the painting materials associated with the deteriorated paint layers, the degradation pathway would involve the interaction between zinc white pigment and oleo-resinous mediums. Reflectance FTIR spectra (Figure 10) acquired from from distinct degraded colors show a band around 1540 cm^{-1} assigned to carboxylate [29]. A weaker absorption around 1315 cm^{-1} also suggests the presence of zinc oxalates [30]. These compounds confirm the involvement of zinc-based degradation products; however, the morphological features of deterioration observed diverge from classical cases of zinc soap aggregation and migration commonly encountered in oil paintings [31,32].

Interestingly, it has been shown that the chemical reactivity of zinc white pigments is not uniform and depends on its mode of synthesis [33,34]: ZnO pigments produced via the direct (American) process typically exhibit intense green photoluminescence under UV excitation, while those produced through the indirect (French) process emit lower-intensity purple-blue fluorescence. During manufacturing, due to elevated temperature, numerous metal atoms can be incorporated into the zinc oxide crystal lattice, leading to significant alterations in its properties. Pigments produced by the direct process typically exhibit near-stoichiometric ratios of zinc to oxygen, whereas those manufactured by the French process are more prone to contain interstitial zinc. A notable consequence of these

structural differences is their influence on UV fluorescence behavior: stoichiometric zinc oxide generally displays a bright green fluorescence, while zinc oxide containing interstitial zinc tends to show a weaker purple-blue fluorescence [35]. In Dalí's painting, undamaged zinc-white-rich areas exhibit photoluminescence behavior consistent with the indirect process (Figure 2c). In this regard, it is important to point out that the indirect preparation procedure may introduce zinc interstitial defects that promote the photocatalytic activity of zinc oxide [36].

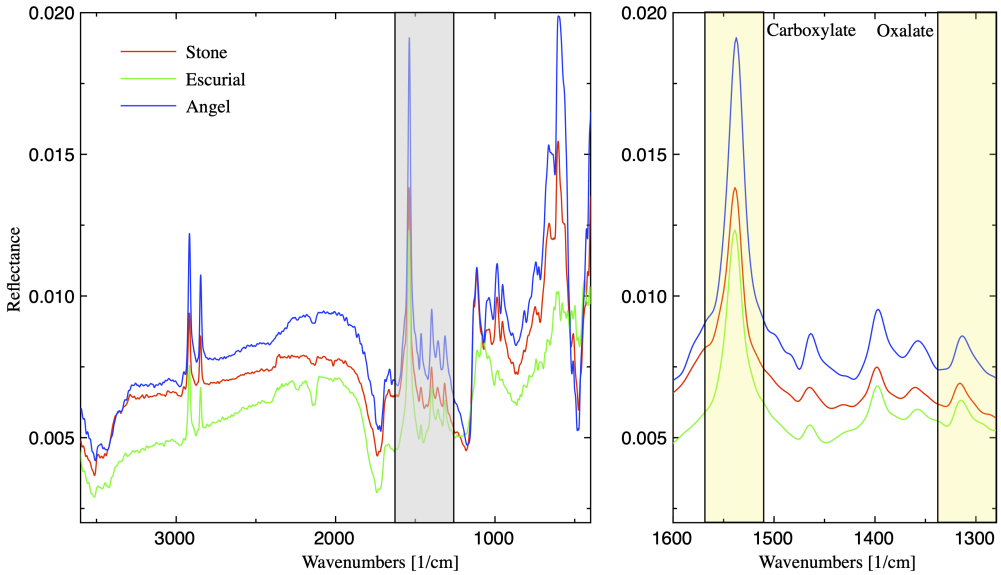

Figure 10. FT-IR bands assigned to carboxylate and oxalate, respectively, observed at ca. 1540 cm^{-1} and ca. 1315 cm^{-1} in the spectra recorded from distinct degraded colors.

Conversely, zones exhibiting degradation present an intense bluish-white luminescence under UV light (Figure 2c), corresponding to increased emission in the 385–415 nm range. However, this emission pattern has been associated with binder deterioration in ZnO-containing systems [14]. The elevated luminescence suggests the formation of zinc-related defect structures—interstitial Zn ions or oxygen vacancies—which are known to enhance the photocatalytic activity of ZnO [37,38]. This activity promotes oxidative degradation of adjacent organic components, accelerating the breakdown of the oleo-resinous medium and potentially contributing to the discoloration or destabilization of co-pigments. Among the various co-pigments found out in deteriorated zones, ultramarine is the only one exhibiting clear signs of discoloration. This may reflect its greater sensitivity to oxidative degradation in the presence of zinc white and oleo resinous binder.

The X-ray diffraction (XRD) measurements performed on deteriorated surfaces highlighted the prevalence of amorphous degradation products, as shown by the increased X-ray scattering at low angles (Figure A6). This finding aligns with previous studies indicating that interactions between metal ions and natural resins often lead to non-crystalline metal–resinate complexes [25,26]. As claimed in *50 Secrets*, Dalí intentionally increased the proportion of dissolved amber in the upper paint layers, aiming for optical richness and luminosity. However, the interaction between terpenoid resin acids from amber and zinc ions may have initiated early-stage reactions during the drying and curing of the paint film.

Prior research [25,26] tends to demonstrate that terpenoid acids are more reactive than fatty acids of drying oils, given their higher mobility. Consequently, in zinc-white-rich systems, zinc ions preferentially react with mobile resin acids—such as those from amber—over triglyceride-derived fatty acids, leading to the formation of amorphous zinc–resinate complexes. These reaction products likely account for the atypical aspect of the affected

areas, which lack the soap protrusions typically found in conventional oil paintings and which differ from the zinc-white-related deterioration reported for Dali's *Couple with Clouds in their Heads* dated 1936 [39,40].

Further experimental studies have outlined the distinct reactivity of natural resins, including colophony, shellac, copal and mastic, and their varying affinities toward different cations from pigments. Nonetheless, the ageing behavior of pigmented films combining oil and amber resin is a topic that has never been investigated so far.

Another critical factor is the presence of lead-white-rich underlayers. Previous studies have highlighted the preferential saponification of zinc oxide over lead carbonate [41–43]. This suggests that lead white from the subsurface could have promoted the reactions between ZnO and active resin acids of amber in the superimposed layers. This seems even more likely if one takes into consideration the uncompleted curing process of the lead-white-based layers in question, since uncured paint systems greatly facilitate the mobility of active metal ions of pigments. By contrast, the titanium dioxide (anatase)-based ground layer does not appear to contribute significantly to the chemical destabilization, further emphasizing the harmful catalytic role of lead white in the present case.

In addition, the MA-XRF results showed a spatial correlation between the zinc and chlorine elements. The increasing intensity of chlorine signals detected in both degraded and non-degraded Zn white layers likely reflects zinc oxide's known affinity for halides. Although previous studies showed that lead white pigments may involve chlorine compounds [44], the detection of chlorine signals on the overall painting surface even in lead-white-free areas suggests an environmental contamination. This assumption is supported by chlorine detection on the original wooden frame via pXRF analyses (Figure A7). Shortly after being exposed in New York city, Dali's St. Anthony was shipped across the Atlantic to be shown in Europe, notably in Brussels in June 1947. One plausible scenario is therefore a contamination resulting from the maritime transport of the artwork. During this early transoceanic transport, the painting may have been exposed to the seawater environment rich in hygroscopic and corrosive chloride salts, such as NaCl. Such exposure would have undoubtedly compromised the stability of the still-curing oleo-resinous paint layers, particularly those containing zinc white. The impact of chloride compounds on ZnO-containing paint systems has been described in the corrosion literature [45], underscoring their ability to disrupt binder matrices and promote further reaction pathways.

4. Conclusions

The historical and multi-analytical study of *The temptation of St. Anthony* has revealed a complex interplay of material, technique, and environmental factors contributing to the painting's current altered state. The observed deterioration patterns were shown to result probably from degradation phenomena rather than solely intentional aesthetic effects. The outcomes achieved underscore the critical role of materials chosen by Dalí—specifically, the combination of zinc white and amber-based medium in the upper layers—and how their interactions may have drastically impacted the appearance of the painting at a very early stage of the aging process.

The possible crystal defects of the zinc white used by Dali may have increased the photocatalytic activity of zinc ions, promoting the decomposition of organic fractions of the oleo-resinous binder. Degraded areas involve both species, zinc carboxylates and zinc oxalates. However, the preferential formation of amorphous zinc–resinate complexes involving terpenoid acids from amber, rather than classical zinc soaps deriving from fatty acids of drying oils, likely accounts for the atypical degradation symptoms observed—transparency, roughness, and discoloration—distinct from previously documented zinc-soap-related

deterioration. Further investigations on laboratory-prepared mockups should allow the hypothesis on the degradation mechanisms proposed by the authors to be validated or refuted.

Furthermore, the stratigraphic configuration of zinc-white/amber-based layers over not fully cured lead-white-rich layers appears to have significantly affected the degradation behavior of the superimposed layers. The catalytic role of lead ions, known to promote zinc soap formation, was likely exacerbated by the mobility of metal ions in uncured paint systems. In contrast, zinc-white-based colors directly applied onto the titanium-white-based ground do not display visible signs of damage, emphasizing the decisive influence of interlayer interactions.

While chlorine was identified across the painting surface, the intensity of the related signals significantly increases only in zinc-white-rich areas. The detection of chlorine on the original frame supports the hypothesis of an exposure to chloride sources post execution. Chlorine contamination may have taken place during the painting's transatlantic transport in 1947. If that were the case, chloride ions from seawater, coupled with high ambient humidity, would have undoubtably compromised the stability of fresh paint films.

To sum up, we can say that the in-depth study of *The temptation of St. Anthony* permitted unprecedented outcomes to be achieved on the degradation behavior of amber-based paint layers, particularly in presence of zinc white.

Author Contributions: Conceptualization, C.D. and D.S.; methodology, C.D. and D.S.; validation, C.D., F.V., P.W., F.C.I. and D.S.; formal analysis, C.D., P.W., E.D., N.d.V., D.A., F.C.I. and D.S.; investigation, C.D., P.W., E.D., N.d.V., D.A. and D.S.; data curation, C.D., P.W., D.A., F.C.I. and D.S.; writing—original draft preparation, C.D.; writing—review and editing, C.D., F.V., P.W., F.C.I. and D.S.; supervision, C.D.; project administration, C.D., F.V. and D.S.; funding acquisition, C.D., F.V. and D.S. All authors have read and agreed to the published version of the manuscript.

Funding: This research was funded by the Belgian Science Policy Office (BELSPO, Brussels) through the FED-tWIN project Face to Face (FED-tWIN2019-prf060).

Data Availability Statement: The data reported in this paper are available from the authors on reasonable requests.

Acknowledgments: The authors sincerely thank Kim Oosterlink, General Director of the RMFAB, for his commitment that greatly assisted this research. The authors would also like to express their gratitude to Véronique Cardon, head of the Archives of Contemporary Art of Belgium (RMFAB); Jelle Van Seghbroeck, photographer at the RMFAB; and Ludovic Godfrin, Modern painting collection keeper at the RMFAB. The authors would like to thank Valentina Pintus and Teodora Raicu from the Institute for Natural Sciences and Technology in the Arts at the Academy of Fine Arts Vienna for the the Py-GC-MS measurements.

Conflicts of Interest: The authors declare no conflicts of interest.

Abbreviations

The following abbreviations are used in this manuscript:

CEA	Centre Européen d'Archéométrie
RMFAB	Royal Museums of Fine Arts of Belgium
LAMS	Laboratoire d'Archéologie Moléculaire et Structurale
MA-XRF	Macro X-Ray Fluorescence
FTIR	Fourier Transform-Infra Red spectroscopy
XRD	X-Ray Diffraction
Py-GC-MS	Pyrolysis–Gas Chromatography–Mass Spectrometry
TMAH	Tetramethylammonium Hydroxide
UV	Ultraviolet

Appendix A. Position of Spot Measurements

Figure A1. Position of the RS measurements (label in red is from the edge of the painting).

Figure A2. Position of the FTIR measurements.

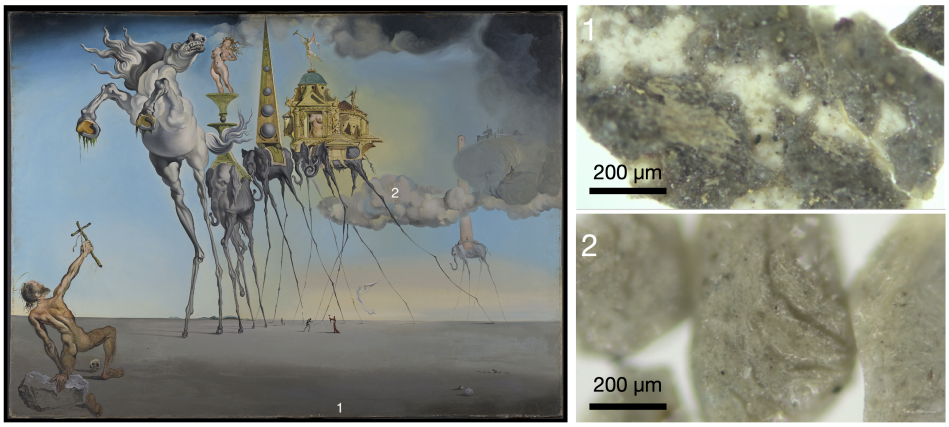

Figure A3. Position and optical microscopy of the micro-samples.

Appendix B. Supplementary Data

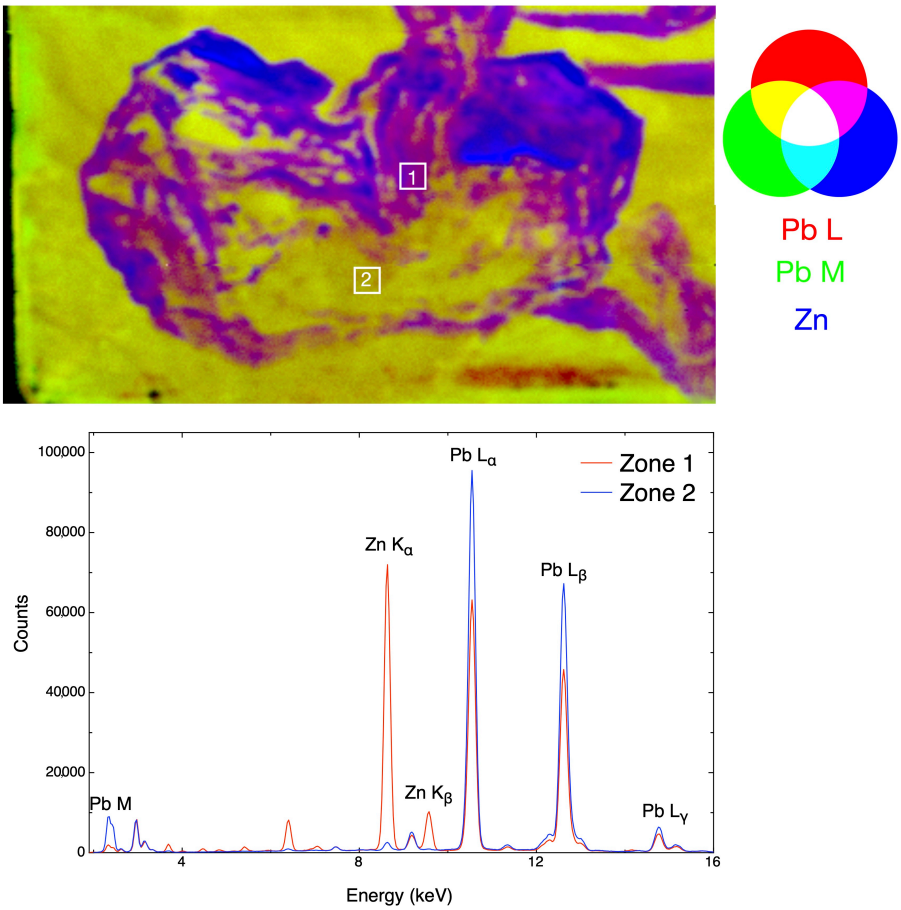

Figure A4. Imaging of the Pb L, Pb M and Zn K lines in the stone supporting St. Anthony showing that the Zn layer is above the Pb layer as there is a high correlation of Pb L and Zn but not with Pb M. High levels of Pb M correspond to regions of lead white on the surface. Comparison of the XRF spectra from regions with Zinc (Zone 1) and without (Zone 2) confirms this hypothesis as the Pb M line is very low in Zone 1 compared to Zone 2 and that the absorption of the L lines is different.

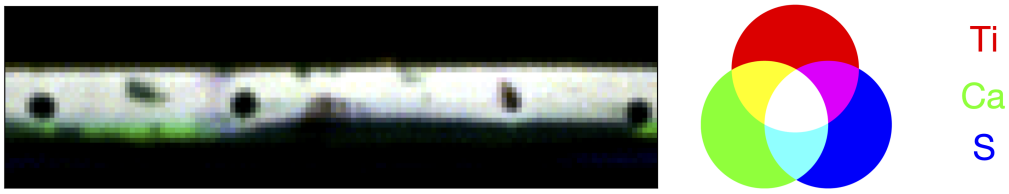

Figure A5. MA-XRF of the exposed ground in a tacking margin showing the presence of titanium (Ti), calcium (Ca) and Sulfur (S), showing the presence of TiO_2 and $CaSO_4$.

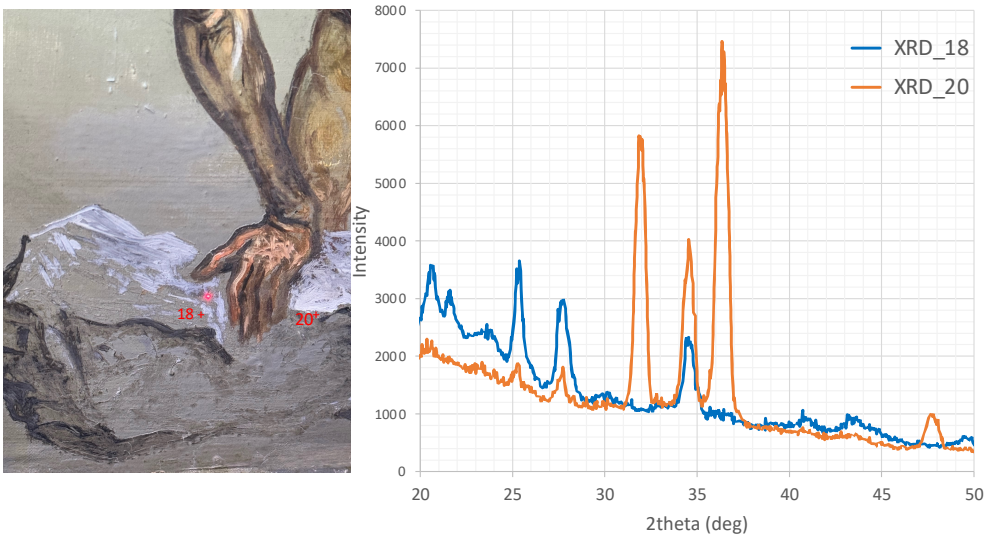

Figure A6. XRD diffractograms of degraded and non-degraded areas in the stone supporting St. Anthony. Dali18: lead white with more important X-ray scattering at low angles due to the presence of an amorphous phase (Cerussite: PDF 47-1734, Hydrocerussite: PDF 75-0991). Dali 20: lead white (Cerussite: PDF 47-1734, Hydrocerussite: PDF 75-0991) and zincite (PDF 36-1451).

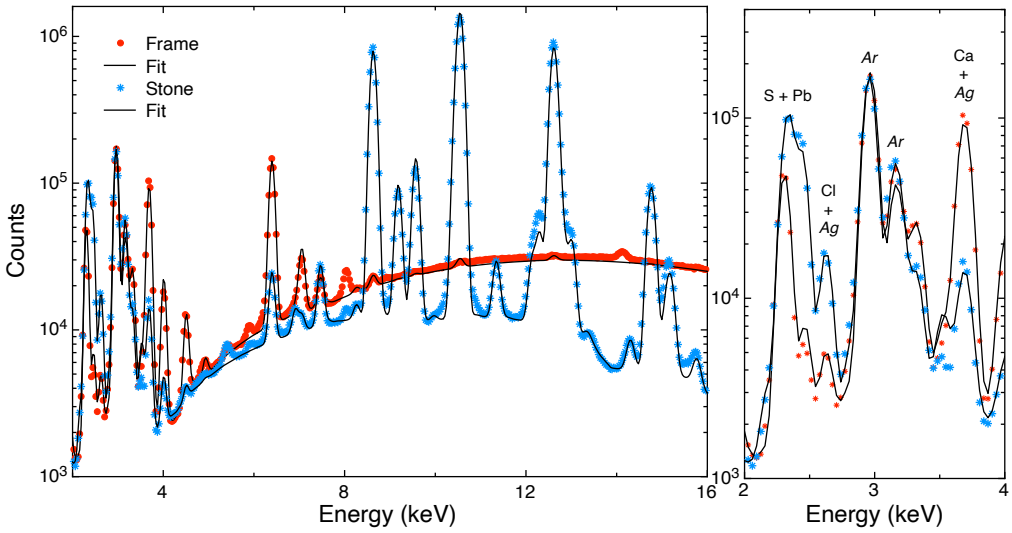

Figure A7. XRF spectra from the stone supporting St. Anthony and from the frame showing the presence of a Cl peak.

References

1. The Temptation of St. Anthony—Bel Ami International Competition and Exhibition of New Paintings by Eleven American and European Artists. In *Magazine of Art 1946–1947*; American Federation of Arts: New York, NY, USA, 1953; Volume 46. Available online: https://archive.org/details/sim_magazine-of-art-1949_1946-1947_46_supplement/mode/2up (accessed on 12 November 2025).
2. *Onze Peintres Interprètent La Tentation de Saint Antoine, le Concours Bel-Ami, Catalog of the Exhibition*; Editions de la Connaissance: Brussels, Belgium, 1947.
3. Dalì, S. *50 Secrets of Magic Craftsmanship*; Dial Press: New York, NY, USA, 1948.
4. Strivay, D.; Clar, M.; Rakkaa, S.; Hocquet, F.P.; Defeyt, C. Development of a translation stage for in situ noninvasive analysis and high-resolution imaging. *X-Ray Spectrom.* **2016**, *122*, 950. [CrossRef]
5. Hocquet, F.P.; Garnir, H.P.; Marchal, A.; Clar, M.; Oger, C.; Strivay, D. A remote controlled XRF system for field analysis of cultural heritage objects. *Appl. Phys. A* **2008**, *37*, 304–308. [CrossRef]

6. Hocquet, F.P.; Calvo del Castillo, H.; Cervera Xicotencatl, A.; Bourgeois, C.; Oger, C.; Marchal, A.; Clar, M.; Rakkaa, S.; Micha, E.; Strivay, D. Elemental 2D imaging of paintings with a mobile EDXRF system. *Anal. Bioanal. Chem.* **2012**, *399*, 3109–3116. [CrossRef] [PubMed]
7. Sole, A.; Papillon, E.; Cotte, M.; Walter, P.; Susini, J. A multiplatform code for the analysis of energy-dispersive X-ray fluorescence spectra. *Spectrochim. Acta Part B* **2007**, *62*, 63–68. [CrossRef]
8. Lauwers, D.; Hutado, A.; Tanevska, V.; Moens, L.; Bersani, D.; Vandenabeele, P. Characterisation of a portable Raman spectrometer for in situ analysis of art objects. *Spectrochim. Acta Part Mol. Biomol. Spectrosc.* **2014**, *118*, 294–301. [CrossRef] [PubMed]
9. Vandenabeele, P.; Wehling, B.; Moens, L.; Edwards, H.; De Reu, M.; Van Hooydonk, G. Analysis with micro-Raman spectroscopy of natural organic binding media and varnishes used in art. *Anal. Chim. Acta* **2000**, *407*, 261–274. [CrossRef]
10. Menges, F. Spectragryph-Optical Spectroscopy Software 2022. Available online: http://www.eïňĂemm2.de/spectragryph/ (accessed on 12 November 2025).
11. Gianoncelli, A.; Castaing, J.; Ortega, L.; Dooryhée, E.; Salomon, J.; Walter, P.; Hodeau, J.L.; Bordet, P. A portable instrument for in situ determination of the chemical and phase compositions of cultural heritage objects. *X-Ray Spectrom.* **2008**, *37*, 418–423. [CrossRef]
12. Aleccia, D. Characterization and Monitoring Over Time of Oil-Based Pictorial Products Purchased by the Belgian Company Jacques Blockx and Their Use in the 20th Century Painting "The Temptation of Saint Anthony" by Salvador Dalí. Master's Thesis, Università Ca' Foscari Venezia, Venezia, Italy, 2023.
13. *Fonds Emile Langui, Box 52*; Archives de l'Art Contemporain en Belgique: Brussels, Belgium, n.d.
14. Artesani, A.; Gherardi, F.; Nevin, A.; Valentini, G.; Comelli, D. A Photoluminescence Study of the Changes Induced in the Zinc White Pigment by Formation of Zinc Complexes. *Materials* **2017**, *10*, 340. [CrossRef]
15. Izzo, F.C.; Kratter, M.; Nevin, A.; Zendri, E. A Critical Review on the Analysis of Metal Soaps in Oil Paintings. *ChemistryOpen* **2021**, *10*, 904–921. [CrossRef]
16. Casadio, F.; Keune, K.; Noble, P.; Van Loon, A.; Hendriks, E.; Centeno, S.A.; Osmond, G. *Metal Soaps in Art: Conservation and Research*; Springer International Publishing: Cham, Switzerland, 2019. [CrossRef]
17. Romano, C.; Lam, T.; Newsome, G.A.; Taillon, J.A.; Little, N.; Tsang J.S. Characterization of Zinc Carboxylates in an Oil Paint Test Panel. *Stud. Conserv.* **2020**, *65*, 14–27. [CrossRef]
18. Mills, J.S. ;White, R; Gough, J.S. The chemical composition of Baltic amber. *Chem. Geol.* **1984**, *47*, 15–39. [CrossRef]
19. Mills, J.S.; White, R. *Organic Chemistry of Museum Objects*, 2nd ed.; Routledge: New York, NY, USA; Taylor & Francis Group: New York, NY, USA, 1994.
20. Fels, D.C.; de Mayerne, T.; Berger, E.; Sulkowski, J.H. *Lost Secrets of Flemish Painting, Including the First Complete English Translation of the De Mayerne Manuscript*; Alchemist: Hillsville, VA, USA, 2001.
21. Czechowski, F.; Simoneit, B.R.T.; Sachanbifiski, M.; Chojcan, J.; Wolowiec, S. Physicochemical structural characterization of ambers from deposits in Poland. *Appl. Geochem.* **1996**, *11*, 811–834. [CrossRef]
22. Wagner-Wysiecka, E. Succinite, Baltic Amber: A Chemical Masterpiece of Nature. *J. Gems. Gemmol.* **2023**, *25*, 69–87. [CrossRef]
23. Poulain, J. ; Helwig, K. Inside Amber: The Structural Role of Succinic Acid in Class Ia and Class Id Resinite. *Anal. Chem.* **2014**, *86*, 7428–7435. [CrossRef]
24. Blockx, J. *Compendium à L'usage des Artistes Peintres et des Amateurs de Tableaux*; Baschet: Paris, France, 1881.
25. Poli, T.; Piccirillo, A.; Nervo, M.; Chiantore, O. Aging of Natural Resins inPresence of Pigments: Metal Soap and Oxalate Formation. In *Metal Soaps in Art*; Casadio, F., Keune, K., Noble, P., Van Loon, A., Hendriks, E., Centeno, S.A., Osmond, G., Eds.; Springer International Publishing: Cham, Switzerland, 2019; pp. 141–152. [CrossRef]
26. Poli, T.; Chiantore, O.; Diana, E.; Piccirillo, A. Drying Oil and Natural Varnishes in Paintings: A Competition in the Metal Soap Formation. *Coatings* **2021**, *11*, 171. [CrossRef]
27. Poli, T.; Piccirillo, A.; Zoccali, B.; Conti, C.; Nervo, M.; Chiantore, O. The role of zinc white pigment on the degradation of shellac resin in artworks. *Polym. Degrad. Stab.* **2014**, *102*, 138–144. [CrossRef]
28. Doménech-Carbó, M.T.; Kuckova, S.; de la Cruz-Cañizares, J.; Osete-Cortina, L. Study of the influencing effect of pigments on the photoageing of terpenoid resins used as pictorial media. *J. Chromatogr. A* **2006**, *1121*, 248–258. [CrossRef] [PubMed]
29. Hermans, J.J.; Keune, K.; van Loon, A.; Iedema, P.D. An infrared spectroscopic study of the nature of zinc carboxylates in oil paintings. *J. Anal. At. Spectrom.* **2015**, *30*, 1600–1608. [CrossRef]
30. Simonsen, K.P.; Poulsen, J.N.; Vanmeert, F.; Ryhl-Svendsen, M.; Bendix, J.; Sanyova, J.; Janssens, K.; Mederos-Henry, F. Formation of zinc oxalate from zinc white in various oil binding media: The influence of atmospheric carbon dioxide by reaction with $^{1}3CO_2$. *Herit. Sci.* **2020**, *8*, 126. [CrossRef]
31. Russo, S.; Brambilla, L.; Thomas, J.B.; Joseph, E. But aren't all soaps metal soaps? A review of applications, physico-chemical properties of metal soaps and their occurrence in cultural heritage studies. *Herit. Sci.* **2023**, *1*, 172. [CrossRef]
32. Beerse, M.; Keune, K.; Iedema, P.; Woutersen, S.; Hermans, J. Evolution of Zinc Carboxylate Species in Oil Paint Ionomers. *ACS Appl. Polym. Mater.* **2020**, *2*, 5674–5685. [CrossRef]

33. Buxbaum, G.; Pfaff, G. *I*ndustrial Inorganic Pigments; Wiley-VCH Verlag GmbH: Weinheim, Germany, 2005. [CrossRef]
34. Palladino, N.; Occelli, M.; Wallez, G.; Coquinot, Y.; Lemasson, Q.; Pichon, L.; Stankic, S.; Etgens, V.; Salvant, J. An analytical survey of zinc white historical and modern artists' materials. *Herit. Sci.* **2024**, *12*, 47. [CrossRef]
35. Osmond, G. Zinc white: A review of zinc oxide pigment properties and implications for stability in oil-based paintings. *AICCM Bull.* **2012**, *33*, 20–29. [CrossRef]
36. Artesani, A.; Dozzi, M.V.; Toniolo, L.; Valentini, G.; Comelli, D. Experimental Study on the Link between Optical Emission, Crystal Defects and Photocatalytic Activity of Artist Pigments Based on Zinc Oxide. *Minerals* **2020**, *10*, 1129. [CrossRef]
37. Clementi, C.; Rosi, F.; Romani, A.; Vivani, R.; Brunetti, B.G.; Miliani, C. Photoluminescence Properties of Zinc Oxide in Paints: A Study of the Effect of Self-Absorption and Passivation. *Appl. Spectrosc.* **2012**, *66*, 1233–1241. [CrossRef] [PubMed]
38. Artesani, A.; Gherardi, F.; Mosca, S.; Alberti, R.; Nevin, A.; Toniolo, L.; Valentini, G.; Comelli, D. On the photoluminescence changes induced by ageing processes on zinc white paints. *Microchem. J.* **2018**, *139*, 467–474. [CrossRef]
39. Defeyt, C.; Vandepitte, F.; Mazurek, J.; Herens, E.; Strivay, D. Investigation on the Speckles Syndrome Affecting Late 1920s Oil Paintings by René Magritte. In *Conservation of Modern Oil Paintings*; van den Berg, K., Bonaduce, I., Burnstock, A., Ormsby, B., Scharff, M., Carlyle, L., Heydenreich, G., Keune, K., Eds.; Springer International Publishing: Cham, Switzerland, 2019; pp. 255–263. [CrossRef]
40. Keune, K.; Boevé-Jones, G. Its Surreal: Zinc-Oxide Degradation and Misperceptions in Salvador Dalí's Couple with Clouds in Their Heads, 1936. In *Issues in Contemporary Oil Paint*; van den Berg, K., Burnstock, A., de Keijzer, M., Krueger, J., Learner, T., de Tagle, A., Heydenreich, G., Eds.; Springer International Publishing: Cham, Switzerland, 2014; pp. 283–294. [CrossRef]
41. Osmond, G.; Keune, K.; Boon, J. A study of zinc soap aggregates in a late 19th century painting by RG Rivers at the Queensland Art Gallery. *AICCM Bull.* **2005**, *29*, 37–46. [CrossRef]
42. Shimadzu, Y.; van den Berg, K.J. On metal soap related colour and transparency changes in a 19th century painting by Millais. In *Reporting Highlights of the de Mayerne Programme*; Boon, J., Ferreira, E.S.B., Eds.; Netherlands Organisation for Scientific Research: The Hague, The Netherlands, 2006; pp. 43–52.
43. Shimadzu, Y.; Keune, K.; van den Berg, K.J. The effects of lead and zinc white saponification on surface appearance of paint. In *Proceedings of the ICOM Committee for Conservation: Preprints of the 15th Triennial Meeting, New Delhi, India, 22–26 September 2008*; Allied Publishers Pvt Ltd.: New Delhi, India, 2008; Volume II, pp. 626–632.
44. Bijker, I.; Deleu, N.; Darcis, Y.; Janssens, K.; Van der Snickt, G. In search for a new lead white: Understanding the historical production processes for industrial-age lead white pigments (1740–1940). *Dye. Pigment.* **2025**, *235*, 112566. [CrossRef]
45. Auvil, N.C.; Vazquez de Vasquez, M.G.; Allen, H.C. Zinc–Carboxylate Binding in Mixed Octadecanoic Acid and Octadecanol Monolayers on Proxy Seawater Solution Surfaces. *ACS Earth Space Chem.* **2021**, *5*, 2947–2956. [CrossRef]